Parametric Acoustic-based Passive Transponders for Ultra-sensitive Temperature and Temperature-Threshold Sensing

Hussein M. E. Hussein, Luca Colombo, and Cristian Cassella

Dept. of Electrical and Computer Engineering
Northeastern University
Boston, MA, USA
h.hussein@northeastern.edu, c.cassella@northeastern.edu

***Abstract*— In this work, we report a new class of passive acoustic-based transponders (PATs), enabling both continuous and threshold temperature sensing, in a reduced form-factor. These PATs rely, for the first time, on the dynamical features exhibited by high-Q X-cut Lithium Niobate ($LiNbO_3$) acoustic resonators, connected to the output of solid-state parametric frequency dividers (PFDs). The unique dynamics of the PFD boost the temperature sensitivity of the acoustic resonator by orders of magnitude. A threshold input power of $\sim -15\ dBm$ triggers a sub-harmonic oscillation in the PFD which is proportional to the temperature variations. This unique feature makes any temperature data accessible, in real-time, needlessly of expensive transponder architectures.**

Keywords—Temperature Sensing; Acoustic Resonators; Nonlinear Dynamics; Parametric Circuits; Frequency Dividers

I. INTRODUCTION

Recently, much attention has been paid to the development of compact and passive radio-frequency (RF) transponders, like RFID-tags [1], enabling the temperature monitoring of a steadily growing number of different kinds of goods and items [2]–[10]. Such effort has been driven by the growing need to protect specialized equipment, such as those used in manufacturing warehouses and data centers, from undesired increases of their operational temperature. Similarly, the availability of such RF systems can also be beneficial in cold-chain applications [3], where passive inexpensive temperature-threshold systems can enable the prompt identification of any perishables, from food to medicine, suddenly exposed to incompatible temperatures that can be deployed over a large areas. Micro- and Nano-Electromechanical Systems (MEMS/NEMS) are an excellent candidate for ultra-sensitive temperature sensing [10], [11]. Aluminum Nitride (AlN) acoustic resonators are attracting attention for temperature sensing because of the considerable Temperature Coefficient of Frequency (TCF) in addition to the compatibility with the Complementary Metal Oxide Semiconductor (CMOS) fabrication process. However, the sensitivity of these acoustic resonators could eventually be limited by their loaded quality factor (Q) at the frequency of interest.

While different types of passive transponders have been demonstrated for enabling either a continuous or a threshold temperature sensing, none of them can simultaneously address both functionalities and have design characteristics that enable monitoring of thousands of different items due to design constraints.

In this paper, we introduce a novel class of passive acoustic-based transponders (PATs) that leverage the unique dynamics of the Parametric Frequency Dividers (PFDs) to boost the sensitivity of high-Q Lithium Niobate ($LiNbO_3$) acoustic resonators, which can exhibit quality factors exceeding 5,000 around 100 MHz [12] Moreover, our PAT can operate in both the continuous and threshold sensing modes at the same time.

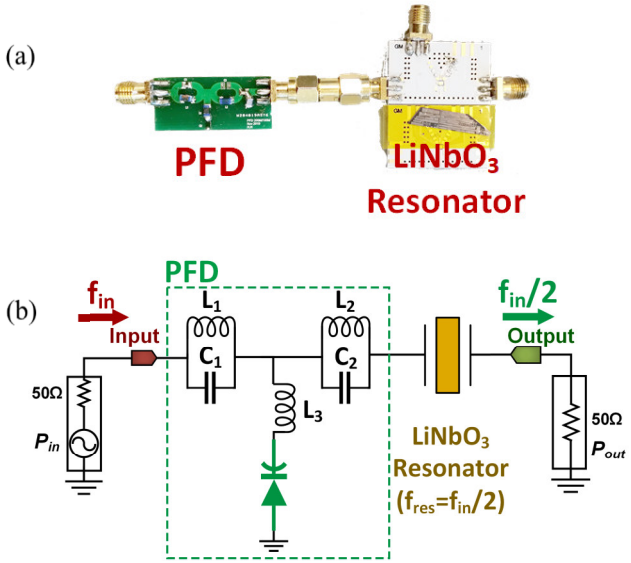

Fig. 1: (a) A picture of the built PAT prototype. (b) A schematic of the PAT showing the PFD circuit and the resonator. Details about the PFD designs are available in [13].

II. THEORY OF OPERATION

The proposed PAT is formed by a varactor-based 2:1 PFD cascaded to an X-cut Lithium Niobate ($LiNbO_3$) acoustic

978-1-6654-3935-0/21/$31.00 ©2021 IEEE

resonator as shown in Fig. 1. The PFD is a two-port RF circuit that is formed by a network of lumped components such as capacitors and inductors together with a solid-state varactor diode [13]. PFDs can inherently activate a 2:1 sub-harmonic oscillation when the input power (P_{in}) exceeds a certain power threshold (P_{th}) through a bifurcation phenomenon. Recently, by investigating the dynamics of the PFD, we realized that the P_{th} of the PFD depends on the impedance seen by the varactor towards the input and the output ports [13]. Therefore, due to the temperature dependance of the $LiNbO_3$ acoustic resonator's resonance frequency, adding the resonator to the output branch of the PFD will consequently result in a shift of P_{th} in response to any temperature variations. The PFD can exhibit two types of bifurcation, either a *super-critical* bifurcation or a *sub-critical* bifurcation depending on the DC-bias (V_{DC}) applied over the varactor. The *super-critical* bifurcation enables a smooth but steep dependence of the PFD output power (P_{out}) *vs.* temperature (T), while the *sub-critical* bifurcation introduces a sudden increase of the P_{out} in presence of small temperature rises. The PFD is strategically engineered to have an input frequency (f_{in}) that is twice the acoustic resonator's resonance frequency at ambient temperature(f_{res}), i.e. $f_{in} = 2f_{res}$. Thus, in case of the *super-critical* bifurcation (the continuous-sensing mode) and by applying P_{in} in proximity to P_{th}, the slightest variation in P_{th} will lead to a significant variation of P_{out}. In other words, the sensitivity of the P_{out} levels *vs.* T variation will be boosted significantly. Similarly, in case of *sub-critical* bifurcation (the threshold-sensing mode) and by applying P_{in} in proximity to P_{th}, the slightest variation in P_{th}will lead to an abrupt increase in the P_{out} level.

The generated P_{out} can be radiated back to the interrogating node, which can receive the information through a different channel from the one used to transmit the signature as shown in Fig. 2. Thus, the PAT is immune to self-interference because the transmitter/receiver communication channels are operating at two separate frequencies.

Fig. 2: PATs using different resonators enable discrimination of the temperature data-streams coming from different items, through dedicated channels that are centered around different lithographically defined f_{res}-values.

III. Results and Discussion

In this work, we built the first prototype of PAT (Fig. 1). This device relies on a lumped PFD assembled on a Printed Circuit Board (PCB) made of FR-4 substrate, using off-the-shelf components. The PFD was designed for a minimum P_{th} ($\sim -15\ dBm$) at $f_{in} \sim 2f_{res}$ ($f_{res} = 108.212\ MHz$). We used an RF signal generator to provide a fixed P_{in} in proximity to the P_{th} with $f_{in} = 216.414\ MHz$, together with a bias-tee and a DC supply to provide the necessary V_{DC} for the proper operational mode. We placed the PAT on a digitally controlled hotplate to sweep T, while simultaneously using a spectrum analyzer to monitor P_{out} at $f_{in}/2$ at the different T values. By applying a $V_{DC} = 0.4\ V$, we can drive the PFD to operate in the super-critical bifurcation mode (continuous-temperature-sensing mode). In Fig. 3, we illustrate the measured normalized P_{out} of the PAT *vs.* T together with the measured normalized transmission coefficient (S_{21}) of the $LiNbO_3$ resonator *vs.* T. As evident from Fig. 3, and thanks to the dynamics of the PFD, P_{out} exhibits a higher sensitivity to T than that exhibited by the S_{21} of the $LiNbO_3$ resonator, operating as a conventional temperature sensor. The measured $LiNbO_3$ resonator's sensitivity is $0.3\ dB/°C$ while the measured PAT's sensitivity is $0.39\ dB/°C$, resulting in a sensitivity boost of 30% with respect to using only the $LiNbO_3$ resonator. In contrast, when applying $V_{DC} = 0.7\ V$, we can drive the PFD to operate in the sub-critical bifurcation mode (temperature-threshold-sensing mode). Similar to the super-critical mode, we fixed P_{in} in proximity to the P_{th} with $f_{in} = 216.414\ MHz$ while maintaining the PAT's temperature equal to the ambient temperature ($25\ °C$). Thanks to sudden dynamics of the PFD in the sub-critical mode, by rising the temperature of the hotplate by only $1\ °C$, this triggers the frequency division mechanism and we are able to obtain an abrupt surge in P_{out} as shown in Fig. 4. Furthermore, to ensure that the sub-critical bifurcation is truly triggered by the $1\ °C$ rise of temperature and is not triggered by the power supply fluctuations, we repeated the measurements four consecutive times by allowing the PAT to heat up until it triggers the sub-critical bifurcation and then we allow it to cool down to its ambient temperature at $25\ °C$ until it reaches the steady state. From Fig. 4, it is evident that the temperature rise of $1\ °C$ is the triggering parameter over the four consecutive cycles.

IV. Conclusions

In this work we introduced a novel parametric acoustic-based temperature sensor. By leveraging both the unique dynamics of parametric frequency divider together with the high temperature coefficient of frequency of the $LiNbO_3$ resonator, we were able to show a boost in the temperature sensitivity compared to what is attained through using only the $LiNbO_3$ resonator. We demonstrated that our system can operate in both the continuous and threshold sensing modes by applying the proper DC bias.

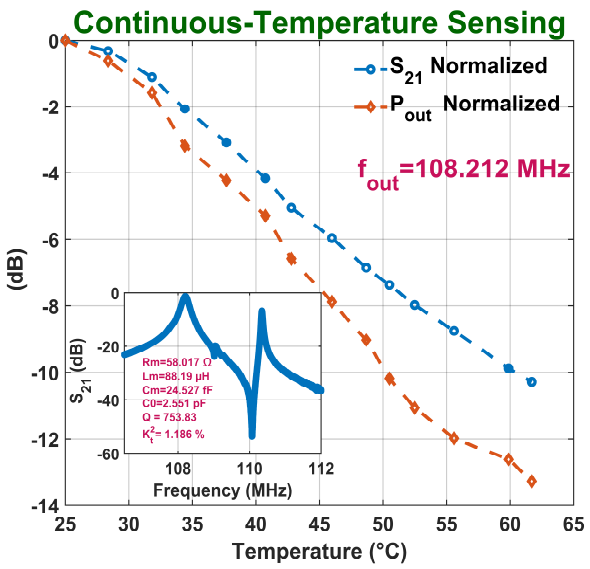

Fig. 3: Measured trends of the normalized PAT output power (P_{out}, in red) vs. T and of the resonator S_{21} vs. T (in blue), for $V_{DC} = 0.4$ V. The measured S_{21} of the $LiNbO_3$ resonator and its equivalent MBVD parameters, at ambient temperature, are also reported. Both trends were extracted after varying the T-value, at the PAT location, through a reprogrammable hot-plate.

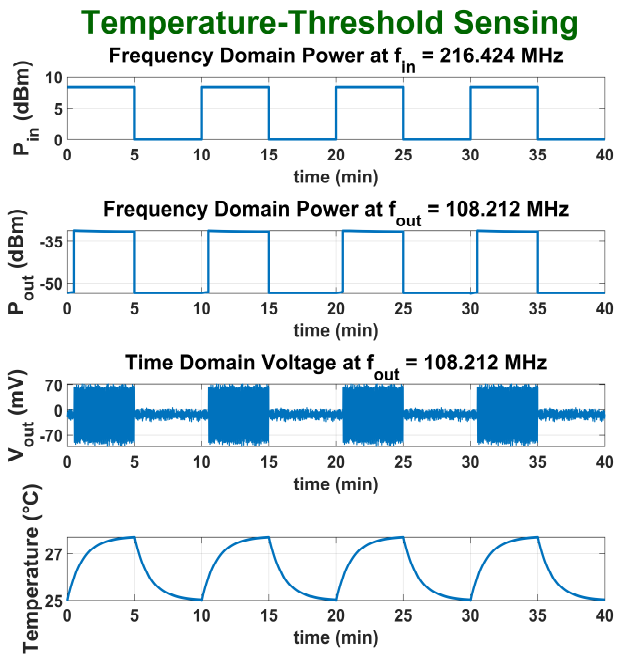

Fig. 4: Frequency-domain trends of $P_{in}(@f_{in})$ and of the measured P_{out} $(@f_{in}/2)$ within a 40 minutes time-frame, including 4 temperature triggering events. Also, a time-domain representation of the PAT output voltage (V_{out}), is reported. Finally, the controlled time-domain temperature profile, at the PAT location that is used in this experiment, is also reported.

REFERENCES

[1] L. M. Ni, Y. Liu, Y. C. Lau, and A. P. Patil, "LANDMARC: Indoor location sensing using active RFID," *Proc. 1st IEEE Int. Conf. Pervasive Comput. Commun. PerCom 2003*, pp. 407–415, 2003.

[2] H. M. E. Hussein, M. Rinaldi, M. Onabajo, and C. Cassella, "A chip-less and battery-less subharmonic tag for wireless sensing with parametrically enhanced sensitivity and dynamic range," *Sci. Rep.*, vol. 11, no. 1, pp. 1–11, 2021.

[3] H. M. E. Hussein, M. Rinaldi, M. Onabajo, C. Cassella, M. Rinaldi, and M. Onabajo, "Capturing and recording cold chain temperature violations through parametric alarm-sensor tags Capturing and recording cold chain temperature violations through parametric alarm-sensor tags," vol. 014101, no. June, 2021.

[4] H. M. E. Hussein and C. Cassella, "Giant Sensitivity through Fully-Passive and Chip-Less Parametric Temperature Sensors," *Proc. IEEE Sensors*, vol. 2020-Octob, pp. 0–3, 2020.

[5] A. Jimenez-Saez, P. Schumacher, K. Hauser, M. Schusler, J. R. Binder, and R. Jakoby, "Chipless Wireless High Temperature Sensing Based on a Multilayer Dielectric Resonator," *Proc. IEEE Sensors*, vol. 2019-Octob, pp. 1634–1637, 2019.

[6] C. Ghouila-Houri *et al.*, "MEMS high temperature gradient sensor for skin-friction measurements in highly turbulent flows," *Proc. IEEE Sensors*, vol. 2019-Octob, pp. 4–7, 2019.

[7] T. T. Thai *et al.*, "Design and development of a novel passive wireless ultrasensitive RF temperature transducer for remote sensing," *IEEE Sens. J.*, vol. 12, no. 9, pp. 2756–2766, 2012.

[8] I. Zalbide, E. D'Entremont, A. Jiménez, H. Solar, A. Beriain, and R. Berenguer, "Battery-free wireless sensors for industrial applications based on UHF RFID technology," *Proc. IEEE Sensors*, vol. 2014-Decem, no. December, pp. 1499–1502, 2014.

[9] R. Bhattacharyya, C. Floerkemeier, and S. Sarma, "RFID tag antenna based temperature sensing," *RFID 2010 Int. IEEE Conf. RFID*, pp. 8–15, 2010.

[10] H. Campanella, M. Narducci, S. Merugu, and N. Singh, "Dual MEMS Resonator Structure for Temperature Sensor Applications," *IEEE Trans. Electron Devices*, vol. 64, no. 8, pp. 3368–3376, 2017.

[11] H. Fatemi, M. J. Modarres-Zadeh, and R. Abdolvand, "Passive wireless temperature sensing with piezoelectric MEMS resonators," *Proc. IEEE Int. Conf. Micro Electro Mech. Syst.*, vol. 2015-Febru, no. February, pp. 909–912, 2015.

[12] L. Colombo, A. Kochhar, G. Vidal-Alvarez, and G. Piazza, "High-Figure-of-Merit X-Cut Lithium Niobate MEMS Resonators Operating around 50 MHz for Large Passive Voltage Amplification in Radio Frequency Applications," *IEEE Trans. Ultrason.*

Ferroelectr. Freq. Control, vol. 67, no. 7, pp. 1392–1402, 2020.

[13] H. M. E. Hussein, M. A. A. Ibrahim, G. Michetti, M. Rinaldi, M. Onabajo, and C. Cassella, "Systematic synthesis and design of ultralow threshold 2:1 Parametric frequency dividers," *IEEE Trans. Microw. Theory Tech.*, vol. 68, no. 8, pp. 3497–3509, 2020.